# Green-Synthesized Silver Nanoparticle Incorporated Poly (para-phenylenediamine)/MWCNT Conductive Nanocomposite for Enhanced Antibacterial Activity and Photocatalytic degradation of Methylene Blue Dye

Laveeza Bano[1†], Ishaat M. Khan*[1], Mohd Imran Ahamed[1†], Rihan[1], Maidul Islam[1,2], Mohammad Khalid Parvez[3], Xiang Li[4]

[1]*Department of Chemistry, Faculty of Science, Aligarh Muslim University, Aligarh 202002, India*

[2]*Divisions of Research and Development Cell, Lovely Professional University, Phagwara, Punjab, 144411, India*

[3]*Department of Pharmacognosy, College of Pharmacy, King Saud University, Riyadh 11451, Saudi Arabia*

[4]*Jiangsu Key Laboratory of Pesticide Science and Department of Chemistry, College of Science, Nanjing Agricultural University, Nanjing, 210095, China*

***Corresponding author.**

**Email address:** drishaatamu@gmail.com (IM Khan)

**† Both authors are first and contributed equally.**

**S1. Synthesis of Polymers**

In the below experiment, polymers are synthesized via chemical oxidative polymerization, in which potassium persulfate has been utilized as an oxidizing agent [1].The main reagents used for the synthesis of the polymer are aniline ($C_6H_5NH_2$) (Fischer Scientific, USA), p-phenylenediamine (99%, SigmaAldrich, USA), m-phenylenediamine (99%, SigmaAldrich, USA), potassium persulfate ($K_2S_2O_8$), conc. HCl (Fischer Scientific, USA). The polymerization of aniline by $K_2S_2O_8$ follows a mechanism similar to the oxidative chemical method, as explained in **Scheme S1**. The synthesis is initiated by drop-wise addition of an oxidant, 0.1M potassium persulphate ($K_2S_2O_8$) in 10% aniline ($C_6H_5NH_2$) prepared in 1M HCl, with continuous stirring by a magnetic stirrer at 1000 rpm for 4-5 hours at 0°C, to complete the polymerization. The synthesized dark green polymer was filtered after being kept at rest for 24h and washed several times with double-distilled water and purified with ethanol [2]**.** The polyaniline was transformed into a fine powder by drying the residue in an oven at 50–60°C for 24 hours, as shown in **Scheme S2** [3]. The polymers of para-phenylenediamine and meta-phenylenediamine were also obtained from their monomers in a similar fashion. The synthesized blue- black precipitate obtained was labelled as poly (p-phenylenediamine), and the black precipitate was labelled as poly (m-phenylenediamine) **(Scheme S2)**.

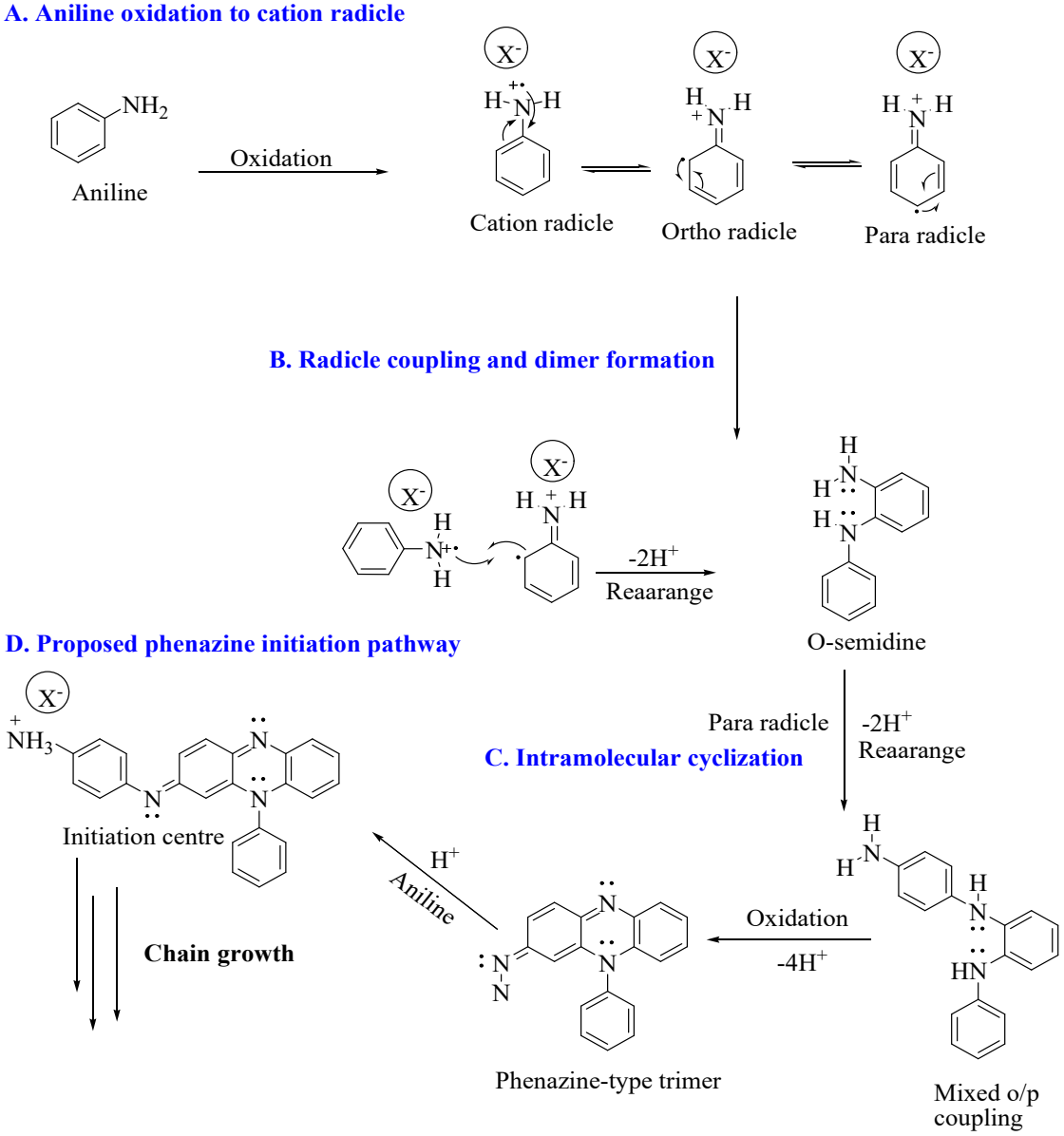


**Scheme S1.** Synthesis of PANI by Chemical Oxidative Polymerization Pathway [4].

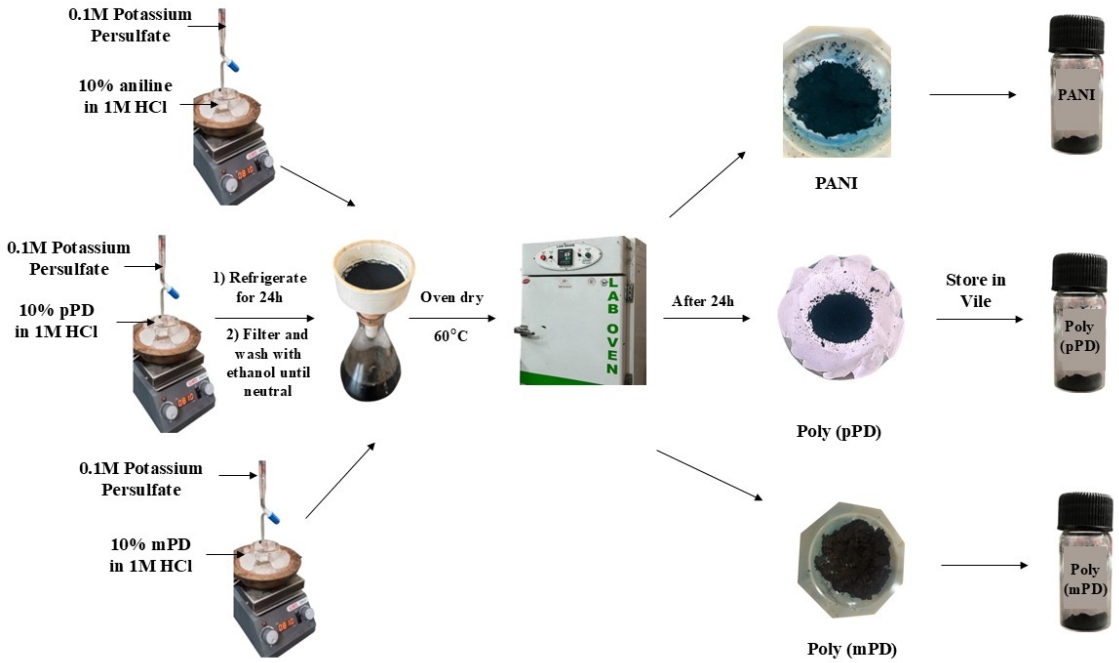


**Scheme S2.** Process of Synthesis of PANI and its derivatives via Chemical Oxidation.

## S2. Characterization of synthesized polymers

### S2.1. FTIR Analysis

The FTIR spectra of PANI, poly(p-phenylenediamine), and poly(m-phenylenediamine) are illustrated in **Fig. S1 (a–c)**. In PANI **Fig. S1 (a)**, the peaks at 1563.67 $cm^{-1}$ and 1482.12 $cm^{-1}$ are assigned to the C=N stretching of quinoid structures and C=C stretching of benzenoid units, respectively, reflecting the oxidation state of the polymer [5]. Bands at 1293.86 $cm^{-1}$ and 1240.15 $cm^{-1}$ arise from C–N stretching vibrations [6] [7]. The intense peak at 1106.28 $cm^{-1}$ indicates delocalized charge carriers along the conjugated backbone, confirming the conductive nature of PANI [8]. Absorptions in the range of 796–879 $cm^{-1}$ are attributed to C–H out-of-plane vibrations [9]. Poly(mPD) **Fig. S1 (b)** shows broad bands at 3328 and 3200 $cm^{-1}$, corresponding to N–H

stretching of secondary amino groups [10]. Peaks at 1617.47 $cm^{-1}$ and 1503.24 $cm^{-1}$ indicate the presence of quinonoid and benzenoid rings, respectively, while the band at 1268.28 $cm^{-1}$ is related to C–N stretching [11] [12]. A weak absorption at 1111.38 $cm^{-1}$ may correspond to C=N stretching [13]. For poly(pPD) **Fig. S1 (c)**, a broad band at 3219 $cm^{-1}$ is linked with N–H stretching. Peaks at 1609.94 $cm^{-1}$ and 1515.06 $cm^{-1}$ reflect N–H bending and C=N stretching, respectively, associated with phenazine-like segments [14]. The peaks at 1423.91 $cm^{-1}$ and 1292.40 $cm^{-1}$ are ascribed with C–N–C stretching vibrations of benzenoid and quinoid imine units. Peaks at 1609.94 $cm^{-1}$ and 1570 $cm^{-1}$ were associated with C–C stretching on the aromatic rings [15]. Further, bands at 1,292.40 $cm^{-1}$, 822.19 $cm^{-1}$, and 1,515.06 $cm^{-1}$ are assigned as C–N aromatic stretching, C–H aromatic stretching, and C=C aromatic stretching bands, respectively [14].

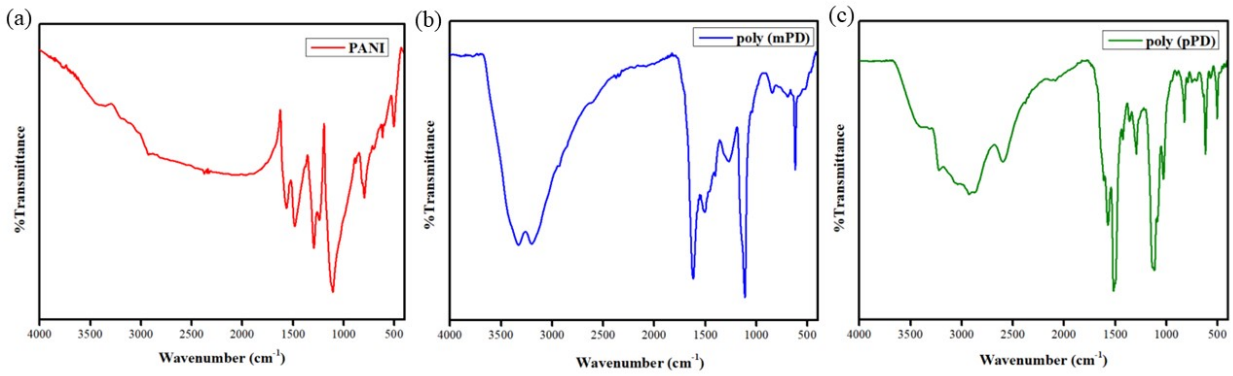


**Fig. S1.** FT-IR Analysis of (a) PANI, (b) poly(*m*-PD), (c) poly(pPD)

**S2.2. PXRD Analysis**

To study the nature of synthesised polyaniline and its derivatives, PXRD was used. XRD spectra of PANI, poly(p-phenylenediamine), and poly (m-phenylenediamine) are shown in **Fig. S2. (a-c).** The PXRD pattern for polyaniline, shown in **Fig. S2 (a)**, reveals a broad peak centered around 2θ ≈ 25°. This indicates amorphous characteristics. This broad feature corresponds to the (200) plane of the emeraldine salt and shows periodicity along the polymer backbone. The absence of sharp

peaks suggests disordered chain packing and limited long-range order. This disorder is typical of chemically synthesized PANI because of irregular chain alignment and structural distortion caused by dopants [16]. The PXRD of poly(meta-phenylenediamine), illustrated in **Fig. S2 (b)**, shows broad and less intense peaks, which indicate a semi-crystalline structure. The meta-substitution disrupts the planarity and linearity of the polymer chains. This reduces the potential for tight π–π stacking and ordered packing. As a result, poly(mPD) shows more structural disorder than its para-counterpart. This leads to broader diffraction features centred around 2θ = 22°–28°, which indicate limited crystalline domains within an amorphous matrix [17]. In contrast, poly(para-phenylenediamine) **Fig. S2 (c)**, displays sharp and intense diffraction peaks in the range of 10°-30°, which can be explained by the structural diversity of the macromolecules of the synthesized polymer and the size and regularity of poly(pPD), indicating its semi-crystalline structure[18] [19]. Moreover, the para-substitution allows linear and planar chain growth, promoting regular π–π stacking and strong intermolecular interactions [20]

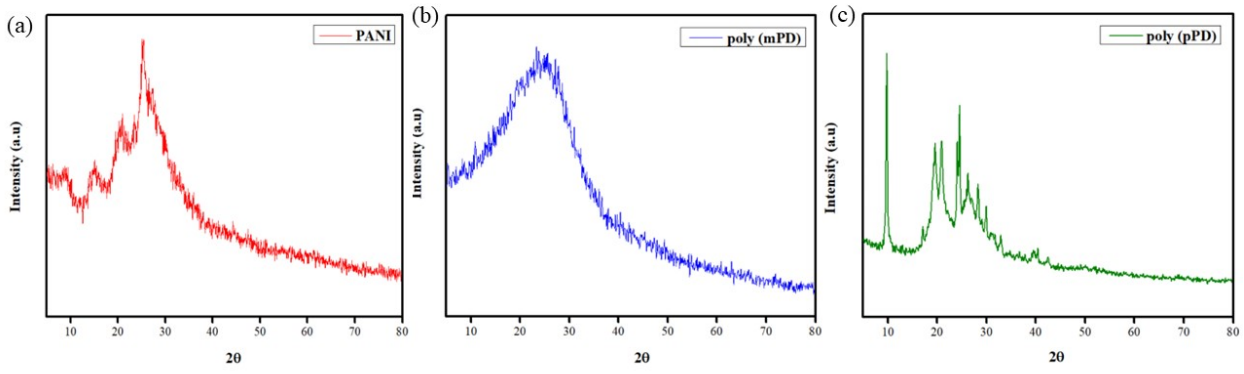


**Fig. S2.** PXRD Analysis of (a) PANI, (b) poly(mPD), (c) poly(pPD)

## *S3. Conductivity Analysis synthesized polymers*

The ionic conductivities of PANI, poly(pPD), and poly(mPD) were investigated in various polar aprotic solvents at room temperature with an ELICO conductivity meter. Aqueous solutions (0.05% w/v) were also measured at room temperature with a Eutech CON 700 meter. Whereas NMP demonstrated the highest conductivity followed by DMF, THF consistently gives the lowest values as shown in **Fig. S3.** The difference in conductivity is probably due to the polarity and dielectric constant of the solvents. Polar aprotic solvents with high dielectric constants, such as NMP and DMF, aid conductivity due to improved solvation and mobility of ions [21]. This trend may also be attributed to the superior solvation and charge transport properties of NMP, which facilitate better polymer chain alignment and higher charge carrier mobility. However, THF's low polarity may limit the dispersion of polymer and ionic conductivity. Overall, NMP is the most effective solvent for achieving high conductivity.

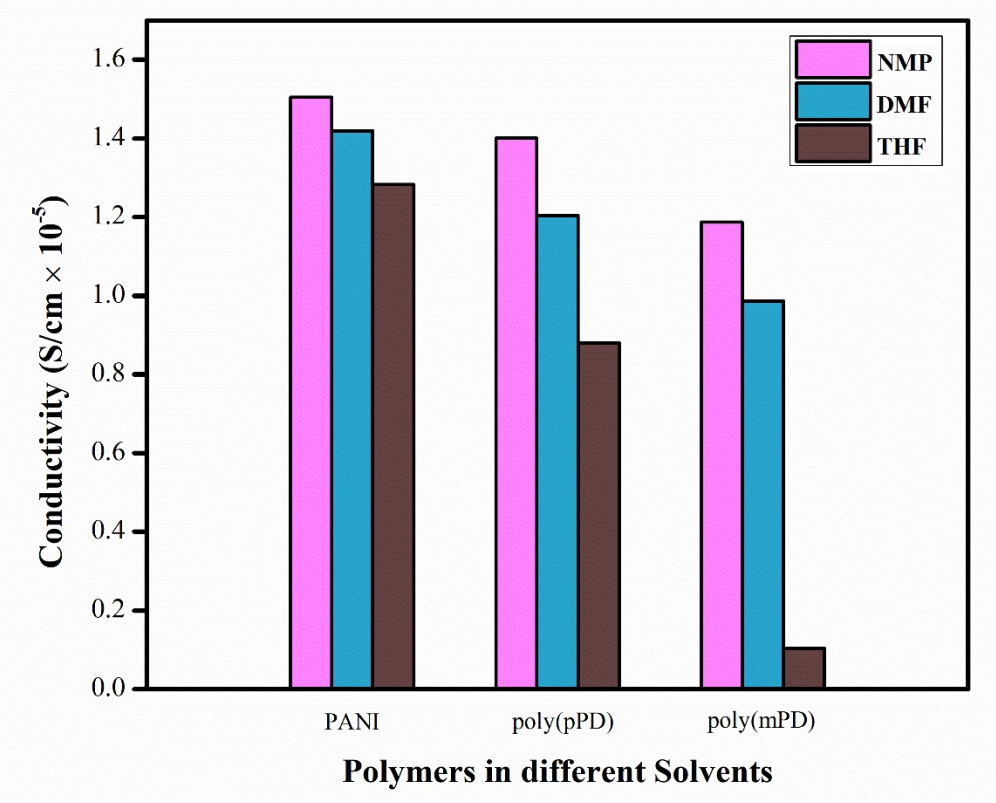

**Fig. S3.** Conductivity of PANI, poly (pPD), and poly(mPD) in different solvents at room temperature.

The electrical conductivity of PANI, poly(pPD), and poly(mPD) was further evaluated varying concentrations of polymers as shown in **Fig. S4**. The results clearly show that PANI possesses the highest conductivity among the three, beginning at $70.0 \times 10^{-5}$ S/cm at 0.715 µg/ml and peaking at $89.7 \times 10^{-5}$ S/cm at 1.144 µg/ml, beyond which it levels off. This trend implies that ideal doping and charge carrier mobility in PANI occurs at 1.144 µg/ml contributing to conductivity [22]. Furthermore, HCl-doped PANI show improved conductivity compared to pure PANI [23]. Poly(pPD), by comparison, has a slower and a more consistent increase in conductivity, increasing from $4.6 \times 10^{-5}$ S/cm to $7.89 \times 10^{-5}$ S/cm, indicating both lower intrinsic conductivity and a less responsive behaviour to volume change. Poly(mPD), on the other hand, consistently showed the poorest conductivity, starting at $1.4 \times 10^{-5}$ S/cm and reaching only $5.5 \times 10^{-5}$ S/cm at high concentration. Bulky $-NH_2$ substituents, which cause twisting of the main-chain, reducing its coplanarity and presenting a barrier to inter-chain jumping and transfer of electrons, which shortens the length of conjugation, likely account for the low electrical conductivity of phenylenediamine polymers [24]. This suggest that its poor electrical performance may be attributed to structural or morphological defect that hinders the proper transport of charge. A bar graph, as shown in **Fig. S4**, illustrates these observations, with PANI at the top for conductivity, followed by poly(pPD) and lastly poly(mPD).

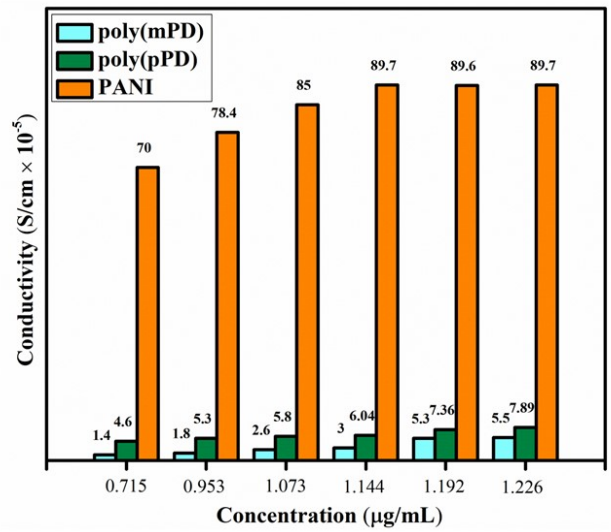


**Fig. S4.** Conductivity measurement of PANI, poly(pPD) and poly(mPD)

## References


1 A. T. Lawal and G. G. Wallace, *Talanta*, 2014, **119**, 133–143.

2 A. A. Khan and Inamuddin, *React Funct Polym*, 2006, **66**, 1649–1663.

3 P. Chaubisa, D. Dharmendra, Y. Vyas, P. Chundawat, N. K. Jangid and C. Ameta, *Polymer Bulletin*, 2024, **81**, 3333–3353.

4 M. R. Saeb, P. Zarrintaj, P. Khandelwal and N. P. S. Chauhan, *Fundamentals and Emerging Applications of Polyaniline*, 2019, 17–41.

5 N. S. Sariciftci, H. Kuzmany, H. Neugebauer and A. Neckel, *J Chem Phys*, 1990, **92**, 4530–4539.

6 J. Tang, X. Jing, B. Wang and F. Wang, *Synth Met*, 1988, **24**, 231–238.

7 T. K. Rout, G. Jha, A. K. Singh, N. Bandyopadhyay and O. N. Mohanty, *Surf Coat Technol*, 2003, **167**, 16–24.

8 K. A. Ibrahim, *Arabian Journal of Chemistry*, 2017, **10**, S2668–S2674.

9 H. Chafai, M. Laabd, M. Elamine and A. Albourine, *Desalination Water Treat*, 2017, **83**, 314–320.

10 I. Amer, D. A. Young and H. C. M. Vosloo, *Eur Polym J*, 2013, **49**, 3251–3260.

11 S. Myler, S. Eaton and S. P. J. Higson, *Anal Chim Acta*, 1997, **357**, 55–61.

12 X. G. Li, W. Duan, M. R. Huang, Y. L. Yang, D. Y. Zhao and Q. Z. Dong, *Polymer (Guildf)*, 2003, **44**, 5579–5595.

13 I. Amer, D. A. Young and H. C. M. Vosloo, *Eur Polym J*, 2013, **49**, 3251–3260.

14 R. Gupta, S. Sanotra, H. N. Sheikh and B. L. Kalsotra, *J Nanostructure Chem*, DOI:10.1186/2193-8865-3-41.

15 J. R. Shanthi, *Synthesis and Characterization of Poly (p-phenylenediamine) in the Presence of Sodium Dodecyl Sulfate*, 2014, vol. 4.

16 S. M. Ambalagi, M. Devendrappa, S. Nagaraja and B. Sannakki, in *IOP Conference Series: Materials Science and Engineering*, Institute of Physics Publishing, 2018, vol. 310.

17 Y. Meng, L. Zhang, L. Chai, W. Yu, T. Wang, S. Dai and H. Wang, *RSC Adv*, 2014, **4**, 45244–45250.

18 R. Rzayev, *SYNTHESIS AND CHARACTERIZATION OF NEW NANO-SIZED POLY(P-PHENYLENEDIAMINE) IN THE PRESENCE OF POTASSIUM PERSULFATE*, .

19 J. R. Shanthi, *Synthesis and Characterization of Poly (p-phenylenediamine) in the Presence of Sodium Dodecyl Sulfate*, 2014, vol. 4.

20 R. Gupta, S. Sanotra, H. N. Sheikh and B. L. Kalsotra, *J Nanostructure Chem*, DOI:10.1186/2193-8865-3-41.

21 S. Palaniappan and C. A. Amarnath, *React Funct Polym*, 2006, **66**, 1741–1748.

22 J. Sannigrahi and S. Majumdar, *AIP Conf Proc*, 2013, **1512**, 938–939.

23 M. Beygisangchin, S. A. Rashid, S. Shafie, A. R. Sadrolhosseini and H. N. Lim, *Polymers (Basel)*, 2021, **13**, 2003.

24 I. Amer and S. Brandt, *Cogent Eng*, 2018, **5**, 1–17.